ASTRO2020 APC White Paper

Orbiting Starshade: Observing Exoplanets at visible wavelengths with GMT, TMT, and ELT

Thematic Area: Planetary Systems

Primary Contact:
Name: [1]John C. Mather
Institution: NASA's Goddard Space Flight Center
Email: John.C.Mather@nasa.gov
Phone: 240-393-3879

Proposing Team:
[1]John Mather, [2]Jonathan Arenberg, [3]Simone D'Amico, [4]Webster Cash, [1]Matthew Greenhouse, [5]Anthony Harness, [1]Tiffany Hoerbelt, [1]Isabel Kain, [7]Wolfgang Kausch, [7,8]Stefan Kimeswenger, [9]Carey Lisse, [10]Stefan Martin, [11,12]Stefan Noll, [1]Eliad Peretz, [7]Norbert Przybilla, [13]Sara Seager, [10]Stuart Shaklan, [14]Ignas Snellen, [10]Phil Willems
(institutions listed at end)

Abstract: An orbiting starshade working with 30-m class ground-based telescopes would enable observations of reflected light from exoplanets at visible wavelengths. Molecular oxygen and water on an exo-Earth could be clearly detected in a 1-hour spectrum out to 7 pc, and its colors could be measured out to 17 pc. The starshade provides the needed contrast and the telescope with advanced adaptive optics provides angular resolution, reduction of the sky background, imaging, and spectroscopy. The necessary starshade orbit is a highly eccentric ellipse, with apogee greater than ~ 185,000 km, to match the observatory velocity, and a different orbit is needed for each target star. Thrust is provided to match the acceleration of the observatory. Based on a JPL Team-X study in May 2019, a ROM cost is $3 B, not including refueling and the possible requirement for a larger launch vehicle. We address the top recommendation of the Exoplanet Science Strategy report [1], that "NASA should lead a large strategic direct imaging mission capable of measuring the reflected-light spectra of temperate terrestrial planets orbiting Sun-like stars."

The orbiting starshade is the newest member of the family of starshades under study with support from the NASA Exoplanets Exploration Program (ExEP). This study was initiated at GSFC in spring 2018, followed by a JPL Team A study in May 2018, the first GSFC science meeting May 14-15, 2019, and a Team X study at JPL the following week. Starshades have been well studied for the Exo-S [2-4], WFIRST [5-11], and HabEx [8, 12-16] missions recently, and in the past for JWST, UMBRAS [17], BOSS [18], New Worlds Explorer [19, 20], and THEIA [21]. We build on that work with a larger and more maneuverable starshade. In principle the orbiting starshade could be designed for compatibility with all telescopes, including future space telescopes like HabEx and LUVOIR, though the details would differ.

1. Introduction: An orbiting starshade would enable ground-based telescopes to observe reflected light from Earth-like exoplanets around sun-like stars. With visible-band adaptive optics, angular resolution of a few milliarcseconds, and collecting areas far larger than anything currently feasible for space telescopes, this combination has the potential to open new areas of exoplanet science. An exo-Earth at 5 pc would be 50 resolution elements away from its star, making detection unambiguous, even in the presence of very bright exo-zodiacal clouds. Earth-like oxygen and water bands near 700 nm could be recognized despite terrestrial interference, with a continuum signal-to-noise ratio of 17 for a 2700 sec exposure and $R = \lambda/\delta\lambda = 150$.

Where did we come from, and are we alone? How do planetary systems form and evolve? Are there planetary systems resembling ours: small rocky planets, an asteroid belt, gas giants, ice giants, and a Kuiper belt? Are there exoplanets similar to Earth, and are there signs of life elsewhere? Are there surface features and weather? To answer these questions, we wish to:

- Obtain multicolor images of entire planetary systems, including outer planets,
- Obtain precise orbits,
- Measure the time dependence of brightness, colors, and spectra,
- Obtain planetary spectra, with spectral resolution optimized for each planet, sensitive to key molecular species (water, oxygen, methane),
- Observe the structure of exo-zodiacal dust clouds (warm and cold), and find planets in bright dust clouds,
- Observe enough targets to probably find an Earth-like planet, since solar system analogs may be rare.

Given the one known example of life, we should look for Earths around Sun-like (F, G, K) stars [1]. While Habitable Zone (HZ) planets around small M stars can be studied with the transit technique, the host stars are very different from ours, with major coronal activity.

2. Key Measurement Objectives: The key measurement objective is to image ~ 12 nearby exoplanetary systems, and obtain orbits and spectra of their planets, in a ~ 3-year prime mission, at visible wavelengths including molecular bands of oxygen, water, and methane. The wavelength range is set by Earth's atmospheric transmission and emission, by the wavelengths of exoplanet molecular bands, and by the maximum size of the starshade. Exoplanet colors can immediately be compared with known solar system objects [22, 23]. Earth stands out in the color-color plot (350/550, 850/550) based on the EPOXI mission data [22], but spectroscopy will always be required.

If we can observe 12 targets, and the fraction of stars having ~ Earth-size planets in the habitable zone is $\eta_\oplus = 0.2$, then there would be $12 \times 0.2 = 2.4 \pm 1.6$ potential Earths suitable for molecular spectroscopy within 7 pc, and we could begin to answer the question of whether they have an atmosphere like ours. Some would be hidden behind the starshade during observations, so this is not a yield calculation. The signature of the exo-molecules would be increased equivalent widths in their absorption bands, above the widths due to telluric interference.

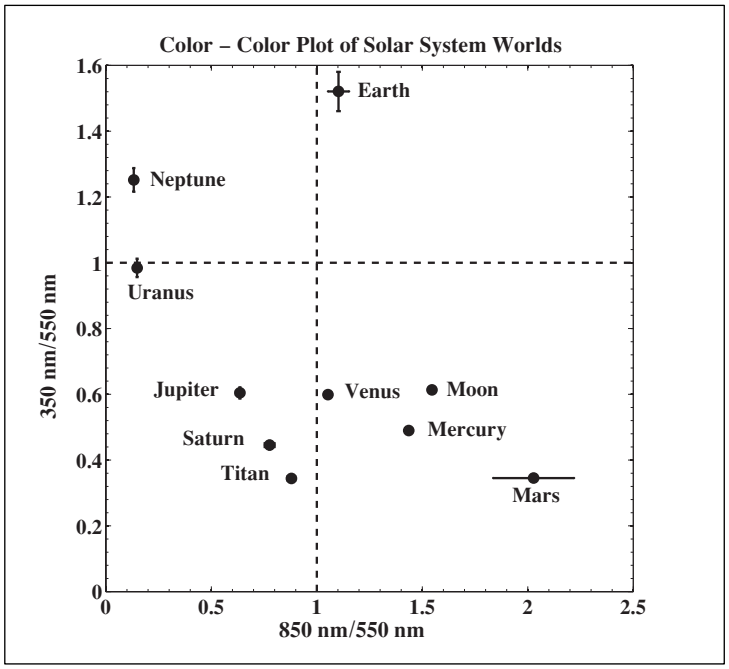

Figure 1. Solar System colors by Crow et al., 2011

2.1 Imaging: The sensitivity and IWA (inner working angle) are sufficient to image a solar system with Venus, Earth, and Mars out to 17 pc in 20 minutes. The IWA is the apparent radius of the starshade seen from the telescope. It is also the angle at which the exoplanet shadow crosses the center of the telescope primary, and the collecting area is cut by about half. If we achieve an IWA of 0.049" there would be ~177 such targets. The telescope response is calculated from the image quality of adaptive optics (Strehl ratio). The telescope resolves the shape of the petals, but the starshade is not in the far field, so its image is blurred. The sensitivity calculation includes the sky background at the telescope, and diffuse light from reflected Earthshine and diffracted starlight from the starshade. With the high angular resolution of large ground-based telescopes, contrast against bright exo-zodiacal clouds is increased in proportion to the square of the aperture; this could be important in the planetary systems with very high exozodiacal brightness, or very clumpy dust.

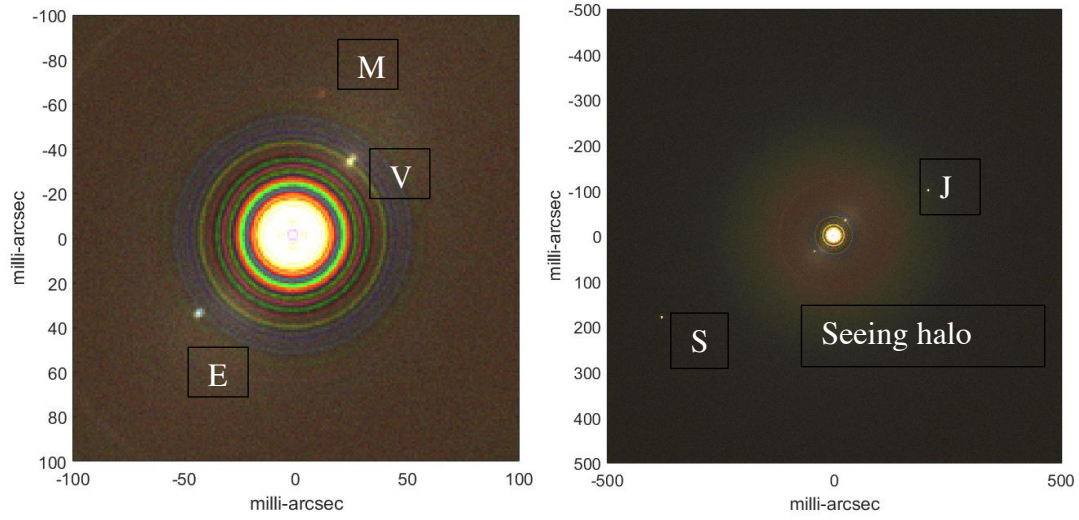

Figure 2. L: Solar System with V=6 star at 17 pc, 20 min exposure, 400-700 nm, exozodi=5x solar system value, system inclined 60°, with Earthshine from 99 m starshade. Mars is at 1:00, Venus at 2:00, Earth at 7:30. R: same with different angular scale. Jupiter and Saturn are at 2:00 and 8:00. Assumed Strehl 0.7, δθ= 3 milliarcsec, seeing disk 0.5". Venus is near IWA.

2.1.1 Planetary Orbits: We need at least three observations to determine an orbit [24, 25]. For M and K stars with small HZs, the orbit may be determined from a single month-long visit. For F and G stars two or three observations up to a month apart in a single visit, plus another 6 months later, may suffice, but would reduce the number observed per year. Precise radial velocity measurements in advance would be extraordinarily valuable.

2.1.2 Time Dependence: We seek evidence of planetary rotation, weather, and surface features by comparing observations at different times. We have a choice of starshade orbit period, as short as 4 days, providing observations of minutes to ~ 1 hour spaced over an observing window of a month or more. Small variations of colors and brightnesses should be evident and molecular spectra may also change.

2.2 Spectroscopy: With the 39 m ELT, we obtain an R=150 visible spectrum of an Earth at 5 pc with a continuum SNR ~ 17 in 2700 sec around 700 nm, reduced to ~ 5 for a 3600 sec exposure at 10 pc. If the measured equivalent widths of the molecular absorption bands are significantly greater than the same bands for the star alone, then exoplanet molecules are detected. Systematic errors are suppressed because: 1) The starshade blocks the starlight geometrically, with high contrast, and the dynamic range is low at the location of the exoplanet image. There is no need to measure a parts-per-million change in brightness as in transit spectroscopy, and no need to suppress the starlight speckles with an actively adjusted coronagraph. For the ELT, an Earth at 5 pc is brighter than the sky background throughout much of the visible band, and we can bring other diffuse backgrounds down to comparable levels. 2) The planetary image is separated by ~50 λ/d from the star for an Earth around a Sun at 5 pc. 3) The atmospheric transmission is measured concurrently with the same spectrometer, using a beacon on the starshade. 4) Reflected Earthshine is diffuse because the starshade is not in focus, and can be compensated by comparing the planet location with neighboring pixels.

We used the online PSG planetary spectrum generator [26], which includes multilayer atmospheres, high resolution spectrum line modeling, and radiative transfer. We propagated the spectra through the Earth's atmosphere using ESO models for Paranal, using ESO models for atmospheric transmission and night-sky radiance (dominated by airglow) at Cerro Paranal (27, 28), and included detector noise, [27, 28], as well as diffuse contributions from reflected Earthshine. In a model exo-Earth, the absorption bands are stronger than for our atmosphere near the zenith, because of the increased path length for the reflected light. Hence, there are portions of each molecular band where the Earth's atmosphere is partially transparent, and the exoplanet is partially absorbing. We detect both oxygen and water if present with concentration and atmospheric pressure like ours, despite terrestrial interference. The molecular lines are collision-broadened, and the opacity in the line wings is proportional to the product of column density and collision rate [29]. Additional factors include high winds, Doppler shifts, and fast rotation. A present-day Earth could be easily recognized, but an atmosphere with low pressure, or with high clouds and haze, would not show terrestrial molecules.

2.3 Target Numbers: Fuel is required to hold the starshade on the line of sight from telescope to star, and to change to a different target star. The rocket equation limits the

number of observable targets [30]. We need high power ion engines, large solar arrays, large fuel tanks, and sufficient time for maneuvers. Observing angle constraints and long maneuvering times combine to give a rate of about 4 targets/year, but this rate may be increased by finding better orbital trajectories and observing strategies. It could also be reduced by staying longer with individual targets to determine exoplanet orbits. Fuel capacities govern the total number accessible before refueling; we budget enough fuel for 12 targets. Refueling 3 times would extend the mission to 12 years and 48 targets.

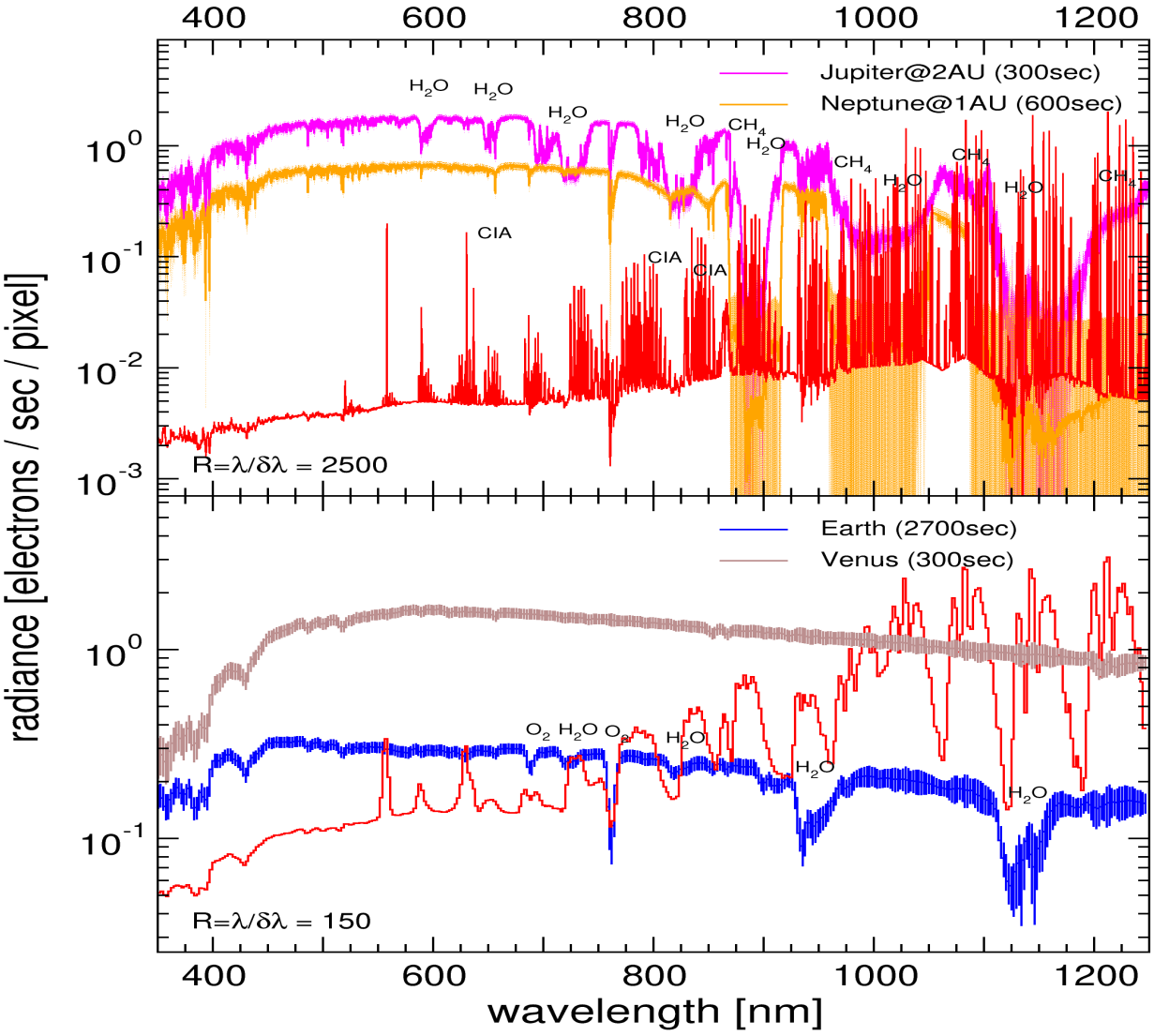

Figure 3. Simulated spectra for planets at 5 pc with Strehl = 0.5. Top panel R = λ/δλ = 2500, bottom R=150. 1 pixel = $\lambda_0/2R$ = 0.14 nm for R = 2000 and 2.34 nm for R = 150 at λ_0 = 700 nm. Red curves are sky brightness at the ELT in Chile. Widths of curves are ± 1σ. Water and oxygen are seen on exo-Earth and not on exo-Venus, and methane registers on a 2 AU Jupiter.

Desired Observation	Metric	Design implication

Colors of planets and comets down to brightness of Mars around Sun-like stars	Contrast 10^{-11} between star and planet, including starshade and telescope	Size, distance, design, and tolerances of starshade; wavelength range
O_2, H_2O in Earth-like planets at 5 pc in 1 hr.	760, 720 nm bands with SNR > 10 and R > 150	Telescope size, Strehl ratio, efficiency, exposure time, Earthshine control
High R general planetary spectra, including CH_4 bands	R > 2500 over at least 500-850 nm	Starshade design, instrument design
Maximize observed targets	12 stars prime mission, up to 2.4 ± 1.6 Earth spectra Objective: 48 stars in 12-year extended mission	IWA ~ 0.049 arcsec (for M stars) Range for Earth spectra 7 pc (sensitivity, exposure time) Maneuvering capability
Exoplanet orbits and variability	3 points covering ≥ 90° of orbit to 0.002" precision	Number & frequency of visits per target
HZ Earth in bright exozodi	~100x capability of WFIRST	Angular resolution, contrast

3. Technical Requirements – Space Segment

The table below summarizes a hypothetical set of mission requirements, without trade studies or optimization, in order to derive a rough cost estimate. The short answer from the Team X study is that there is no known technical reason why such a system could not be built, and the budget for the most challenging item, the deployable starshade itself, is a small fraction of the total.

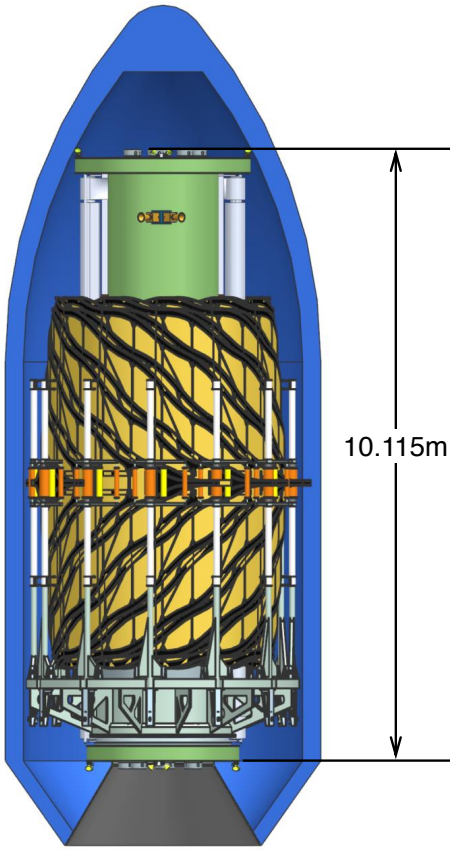

The orbiting starshade is designed to cast a deep shadow and its pointed sunflower shape is chosen based on diffraction calculations [19-21, 31]. The design with a central hub surrounded by tapered petals apodizes the diffraction pattern by approximating a hyper-Gaussian taper of opacity. Shape tolerances are greatly relaxed compared to designs for smaller telescopes, because the telescope itself provides high angular resolution and contrast. The shade is oriented to keep the Sun off the Earth-facing surface, but need not be perpendicular to the line of sight. The shade must be coated or shaped on the Earth-facing surface to minimize reflected Earthshine.

Chemical propulsion is required to hold the starshade on the line of sight during observations, matching the transverse component of the acceleration of the

observatory around the Earth's axis. Since the jets might be luminous enough to interfere with observations, we assume they must be capable of operating in pulsed mode with a duty cycle < 10%, which implies a requirement for up to 5000 N thrust. Solar electric propulsion (SEP) is required for retargeting, since each target-observatory-time combination requires a different orbit, matching the position and velocity to the telescope line of sight at the beginning of an observation. The starshade provides a beacon to support adaptive optics on the ground telescope, and a continuum light source to calibrate the atmospheric transmission at the molecular bands of interest. The beacon is on a gimbal to aim at the telescope within arcseconds, which provides its own beacon as an alignment target. The folded system barely fits the Falcon Heavy fairing in this Team-X concept, and could not accommodate all of the propulsion requirements in the table below.

Item	**Desired values**	**Margin/Remarks**
Orbit type	Highly elliptical Earth orbit Perigee > 1,000 km above surface Distance during observation > 195,000 km N ≥ 4-day period Different orbit for each target	Higher orbits need less maneuvering fuel. Observations need not be at apogee. Integer number of days for repeat observations.
Mission Class	Class A	
Mission Duration	3 yr prime mission, baseline	Objective: 4 x 3 yrs with 3 refueling visits
Starshade central disk	24.75 m radius	Team X baseline, not optimized
Starshade petals	48 petals, 24.75 m long	
Starshade tolerance	Edge shape 5 mm, petal position 5 cm	Looser than for smaller telescopes & starshades
Earthshine reflectance	0.5% (equivalent star mag ~ 22)	Limited by dust contamination
Chemical fuel thruster force	5000 N	~ 10% duty cycle during observation to allow for thruster luminosity
Ion thruster force	4 N	8 AEPS 0.6 N thrusters at a time
Propellants and specific impulse	Biprop (N_2H_2 + N_2O_4), 5000 kg, Isp 280 sec Xenon 3000 kg; Isp 2700 sec	Redesign objectives, did not fit rocket in Team-X study. Global production of xenon in 2015 ~ 53,000 kg.
Dry Mass Launch mass	Dry: 14000 kg CBE + contingency Wet: 22000 kg	Increased fuel from Team X
Maneuvering capability	775 m/s chemical, 3710 m/s Xenon	Objective for redesign
Launch Vehicle (LV)	Falcon Heavy, 22000 kg capacity	Placeholder for future LV
Fairing	4.6 m diam for Falcon Heavy	Too tight
Solar Power	116 kW	Team X baseline

Communication	NEN (Near Earth Network)	
Navigation	High altitude GPS; ground station signal timing	GPS proven on MMS out to 187,000 km; GEONS software
Formation Sensing & control	Acquisition: imaging from observatory camera Science: ±2 m using diffracted starlight in pupil plane imager	Requirements on ground instrumentation and communication Typical 1-minute dead band cycle for pulsed jets
Attitude Control	3-axis stabilized with jets, not rotating	± 1 deg sufficient
Optical systems	Laser beacon for adaptive optics, simulate 8th mag star. Continuum light source to calibrate atmospheric transmission	Like laser comm terminal without the data system, needs gimbal.
Radiation hardness	100 kRad behind 100 mil. of Al	2000 trips through radiation belts

Observing Angle Constraints

Item	**Target value**	**Remarks**
Sun angle from zenith	> 108°	Astronomical night
Target angle from meridian	< 30°	for fuel efficiency, could be extended
Zenith angle	< 60°	for adaptive optics efficiency
Angle from plane to LOS	90° ± 20°	Cosine(Tilt angle) reduces projected shadow size
Sun-Earth-Target angle	< 110°	Wider than prior designs based on tilt
Observing windows	2/year/target 1-9 months long	Depends on target ecliptic latitude and observatory (N or S)
Observations per target	1 + (30 days/orbit period)	Needs trade study
Observation duration	1 hour typical	fuel limited

Propulsion Requirements

Item	Value	Remarks
Stationkeeping Delta V (N-S)	~ 120 m/s/hr $\times \sin(\delta)\cos(\theta)$	δ = declination. Due to observatory acceleration. Zero at equator.
Stationkeeping Delta V (E-W)	~ 120 m/s/hr $\sin(\theta)$	θ = hour angle from meridian. Zero at meridian.
Mean angle between targets	60°	For 12 prime targets; sqrt(4π/N)

Transit time to next target	< 2 months (average)	Allows 4 targets/year
Retargeting Delta V (small moves)	40 m/s/degree for small moves, 4-day orbit	Value for SEP; smaller DV for larger orbit
Retargeting Delta V	300 m/s for large moves via near-escape and return	Budget; free parameter is time; orbit study needed

4. Technical Requirements – Ground Segment: The observatory requires a customized adaptive optics instrument compatible with a laser beacon, but is otherwise similar to designs already being developed for exoplanet studies with VLT [32, 33], Magellan Telescope [34-36], GMT, TMT, and ELT. The instrument must extract the laser wavelength for wavefront sensing, and block the laser light from the camera. Moreover, the starshade and its laser beacon and continuum source are not in the far field, so are not focused in the same plane as the star and planets. We recommend an additional coronagraphic stop at a plane conjugate to the starshade, to block stray light coming from the starshade itself (reflected Earthshine, sunlight scattered on the edges or micrometeoroid punctures or stiffening structure, starlight leaking through punctures, and starlight leaking around the edge). A shutter will close about once/minute while the starshade jets are firing, but their plumes will disappear within milliseconds when the jets are stopped. An IR sensor will image the pupil plane, where the IR starlight diffracted around the starshade can provide a position error signal. An integral field spectrometer surveys an entire exoplanet field at low resolution, and a fiber-fed spectrometer selects planets that are bright enough for higher spectral resolution, or that do not fall within the IFU field of view.

Item	**Baseline**	**Remarks**
Telescopes	24 m GMT, 30 m TMT, 39 m ELT	Source photon noise from an Earth at 5 pc is dominant for ELT
Adaptive optics efficiency	Strehl 0.5 at 700 nm	Requires laser beacon on starshade. Based on MagAO-X plans for zenith Strehl = 0.7.
Block starshade light	Lyot coronagraph; starshade not in far field	Stop starlight leakage, sun glints, Earthshine
Shutter	Block light from stationkeeping jets	Jets could be bright, so jets are pulsed on ~ 1 min cycle. Item for future study.
Diffraction limited camera pixels	Nyquist $\lambda/2D$ = 1.3 milliarcsec	Full spatial resolution for ELT
Camera FoV	7 arcsec radius	Isoplanatic patch; ~ 100 Mpix
Integral field spectrometer	R = 150	Large FoV to capture whole planetary system. Need trade study for R.
Fiber fed spectrometer	R = 150 & R ≥ 2500	For selected planets
Starshade offset sensor	± 1 m resolution	Pupil imaging of starshade IR diffraction

Laser beacon	Target for starshade beacon	

5. Operational Concept:

1. Launch into long elliptical orbit aimed towards top priority target star, phased to line up with observatory at chosen time and date, with correct velocity
2. Set starshade orientation, edge-on to Sun, nearly perpendicular to Line of Sight
3. Set up adaptive optics on ground, locking onto laser beacon, measuring relative position of star and starshade
4. Fine orbit adjustment to within 10 m at 1000 sec from encounter
5. Command starshade to close control loop on starshade position, using chemical thrust, maintain within ± 2 m tolerance to keep shadow dark (using error telemetry from ground)
6. Take multicolor images to identify exoplanet locations
7. Take IFU spectra for central region, OR within minutes, automatically set up fiber fed spectrometer for selected targets
8. Expose ~ 1/2 hr depending on brightness, geometry, priority; ~ 1 hr maximum
9. Command starshade to stop position control, aim orbit for repeat observation or next target, using solar electric propulsion, and repeat as needed
10. When fuel is nearly exhausted, await servicing mission, or aim for safe disposal

6. Technology Drivers: The orbiting starshade shares the technology development items of smaller starshades, currently being managed by the ExEP S5 technology program. Additional items are listed below.

Item	**Value**	**Remarks**
Improved surface to limit Earthshine	0.5% dust coverage assumed	Future study topic
Advanced adaptive optics	Strehl 0.5 assumed	0.7 included in single-conjugate MagAO-X plans for Magellan Telescope
Robotic refueling	Unlimited life extension	In development with GSFC Restore-L, DARPA RSGS, & commercial missions
Ultra-lightweight structure	Existing concepts exceed necessary shape tolerances	Alternatives possibly enabled by relaxed tolerances

A key supporting technology is an orbiting laser beacon to support advanced single-conjugate adaptive optics (SCAO) for all possible targets, all observatories, and all wavelengths including visible and possibly U-band ultraviolet, depending on AO progress and scientific demand. Without active propulsion during an observation, a single beacon can remain in the isoplanatic patch of a chosen target for up to 9000 seconds as shown by Marlow et al. [37]. The coming 30-m class ground-based telescopes will provide facility-level adaptive optics for the entire sky, but only at near-IR wavelengths, using multiple upgoing laser beams. A fleet of orbiting laser beacons would enable an angular resolution 12x better than with Hubble Space Telescope, and 3x better than with near-IR AO, though

with a low duty cycle. The weather could be monitored on all the planets, the heart on Pluto could be resolved, and 30th magnitude stars in nearby galaxies could be imaged in minutes. No other planned technology would provide this capability. A custom-designed SCAO instrument would be required; the beacon is not in the far field, the laser wavelength(s) would be different, and (unlike the starshade) the guide star moves during the observation.

7. Organization, Partnership, and Current Status: The NASA Exoplanets Exploration Program, managed by JPL for NASA Headquarters, Astrophysics Division, is the sponsor of the current work. The work was initiated at Goddard Space Flight Center by John Mather and Eliad Peretz and supported by Goddard internal funds. Contributors to the discussion include representatives of the GMT, TMT, and ELT observatories. Starshade performance was calculated by A. Harness (Princeton) and S. Shaklan (JPL). Simulated images were prepared by S. Shaklan and simulated spectra by S. Kimeswenger et al. (Universität Innsbruck) with support from S. Noll, N. Przybilla, and W. Kausch. Orbit calculations at GSFC were made by S. Hur-Diaz, C. Webster, D. Folta, D. Dichmann, R. Qureshi, and R. Pritchett. We thank R. Campbell, M. Cirasuolo, J. Kasdin, M. Greenhouse, M. Lake, N. Lewis, S. Hildebrandt Rafels, M. Turnbull, G. Villanueva, and K. Warfield for fruitful discussions.

The current technical objective is to complete a mission concept study for comparison with other missions. The Team X study produced a Master Equipment List as a basis for cost and mass calculation, but did not include an actual mechanical design. The starshade itself was scaled from designs for the HabEx starshade. However, even at the concept stage, the orbiting starshade could barely fit the selected Falcon Heavy launch mass capacity and fairing size, and could not observe enough target systems with the available fuel. To increase the number of targets to be visited, we will analyze a refueling option, consider alternate launch vehicles like the SLS and BFR, and attempt to reduce the dry mass to increase maneuverability.

8. Schedule: The Team X cost estimate was based on a launch in 2035. The assumed schedule was 94 months from Phase A through D. This allows for ~8 years of pre-phase A.

9. Cost estimates: The cost estimate was performed by Team X at JPL in May 2019. The base fiscal year was 2019, and the top-level cost was $3.0 B in FY2019 dollars. The cost estimate includes Phase A through launch and 3 years of operation with 30% reserves on the development, and $223M for the Falcon Heavy. The value is a ROM (rough order of magnitude) without a detailed design. The estimate does not include science operations, science community support, instrument development for the ground-based observatory, the technology development effort, or the fleet of orbiting laser beacons to demonstrate advanced adaptive optics. It also does not include the cost of refueling missions, or the possibility of a larger launcher. To estimate refueling costs we consider the International Space Station. The SpaceX Dragon capsule has docked autonomously with the ISS and costs an average of $180 M/flight. The Lunar Gateway Power and Propulsion Element (PPE), with solar electric propulsion, is on contract for a 2022 launch at $375 M, firm fixed price.

Considering all the possible changes from the Team-X concept, the parts not included, and three refueling modules, the total cost could approach $4 B.

Institutions

[1]John Mather, [2]Jonathan Arenberg, [3]Simone D'Amico, [4]Webster Cash, [1]Matthew Greenhouse, [5]Anthony Harness, [1]Tiffany Hoerbelt, [1]Isabel Kain, [7]Wolfgang Kausch, [7,8]Stefan Kimeswenger, [9]Carey Lisse, [10]Stefan Martin, [11,12]Stefan Noll, [1]Eliad Peretz, [7]Norbert Przybilla, [13]Sara Seager, [10]Stuart Shaklan, [14]Ignas Snellen, [10]Phil Willems

[1] NASA, Goddard Space Flight Center, Greenbelt, MD 20771 USA.
[2]Northrop Grumman, One Space Park, R8/2789, Redondo Beach CA 90278
[3]Aeronautics and Astronautics Department, Durand Bldg., Room 262, 496 Lomita Mall, Stanford University, Stanford, California 94305-4035
[4]University of Colorado, Boulder, CO 80309,
[5] Mechanical and Aerospace Engineering, Princeton University, Princeton, NJ 08544, USA
[7] Institut für Astro- und Teilchenphysik, Universität Innsbruck, Technikerstr. 25/8, 6020 Innsbruck, Austria
[8] Instituto de Astronomía, Universidad Católica del Norte, Av. Angamos 0610, Antofagasta, Chile
[9] Johns Hopkins University Applied Physics Lab, 11100 Johns Hopkins Road, Mailstop 200-W230, Laurel MD 20723-6099
[10] Jet Propulsion Lab, California Institute of Technology, 4800 Oak Grove Drive, Pasadena, CA 91109, USA.
[11] Institut für Physik, Universität Augsburg, 86135 Augsburg, Germany
[12] Deutsches Fernerkundungsdatenzentrum, Deutsches Zentrum für Luft- und Raumfahrt, 82234 Weßling-Oberpfaffenhofen, Germany
[13] MIT, Department of Earth, Atmospheric, and Planetary Sciences, 77 Massachusetts Ave., Cambridge, MA 02139
[14]Leiden Observatory, Oort Building, Room 439, Postbus 9513, 2300 RA Leiden, The Netherlands

References

[1] National Academies of Sciences, *Exoplanet Science Strategy*. Washington, DC: The National Academies Press, 2018.

[2] S. Seager *et al.*, "The Exo-S probe class starshade mission," in *Techniques and Instrumentation for Detection of Exoplanets VII*, September 01, 2015, vol. 9605. [Online]. Available: https://ui.adsabs.harvard.edu/abs/2015SPIE.9605E..0WS

[3] S. B. Shaklan *et al.*, "Error budgets for the Exoplanet Starshade (Exo-S) probe-class mission study," in *Techniques and Instrumentation for Detection of Exoplanets VII*, September 01, 2015, vol. 9605. [Online]. Available: https://ui.adsabs.harvard.edu/abs/2015SPIE.9605E..0ZS

[4] R. Trabert *et al.*, "Design reference missions for the exoplanet starshade (Exo-S) probe-class study," in *Techniques and Instrumentation for Detection of Exoplanets VII*, September 01, 2015, vol. 9605. [Online]. Available: https://ui.adsabs.harvard.edu/abs/2015SPIE.9605E..0YT

[5] V. P. Bailey *et al.*, "Lessons for WFIRST CGI from ground-based high-contrast systems," in *Space Telescopes and Instrumentation 2018: Optical, Infrared, and Millimeter Wave*, vol. 10698, M. Lystrup, H. A. MacEwen, and G. G. Fazio Eds., Proceedings of SPIE, 2018.

[6] J. Krist *et al.*, "WFIRST coronagraph flight performance modeling," in *Space Telescopes and Instrumentation 2018: Optical, Infrared, and Millimeter Wave*, vol. 10698, M. Lystrup, H. A. MacEwen, and G. G. Fazio Eds., Proceedings of SPIE, 2018.

[7] B. Lacy, D. Shlivko, and A. Burrows, "Characterization of Exoplanet Atmospheres with the Optical Coronagraph on WFIRST," *Astronomical Journal,* vol. 157, no. 3, Mar 2019, Art no. 132, doi: 10.3847/1538-3881/ab0415.

[8] B. Mennesson *et al.*, "The WFIRST Coronagraph Instrument: a major step in the exploration of Sun-like planetary systems via direct imaging," in *Space Telescopes and Instrumentation 2018: Optical, Infrared, and Millimeter Wave*, vol. 10698, M. Lystrup, H. A. MacEwen, and G. G. Fazio Eds.,(Proceedings of SPIE, 2018.

[9] M. J. Rizzo *et al.*, "WFIRST Coronagraph Integral Field Spectrograph Performance in the OS6 Observing Scenario," in *Space Telescopes and Instrumentation 2018: Optical, Infrared, and Millimeter Wave*, vol. 10698, M. Lystrup, H. A. MacEwen, and G. G. Fazio Eds., Proceedings of SPIE, 2018.

[10] B. J. Seo *et al.*, "Hybrid Lyot Coronagraph for WFIRST: High Contrast Testbed Demonstration in Flight-like Low Flux Environment," in *Space Telescopes and Instrumentation 2018: Optical, Infrared, and Millimeter Wave*, vol. 10698, M. Lystrup, H. A. MacEwen, and G. G. Fazio Eds., Proceedings of SPIE, 2018.

[11] E. Sidick, J. Krist, and I. Poberezhskiy, "WFIRST Coronagraph: Digging Dark-Holes with Partially Corrected Pupil Phase," in *Space Telescopes and Instrumentation 2018: Optical, Infrared, and Millimeter Wave*, vol. 10698, M. Lystrup, H. A. MacEwen, and G. G. Fazio Eds., Proceedings of SPIE, 2018.

[12] B. S. Gaudi *et al.*, "The Habitable Exoplanet Observatory (HabEx)," in *Space Telescopes and Instrumentation 2018: Optical, Infrared, and Millimeter Wave*, vol. 10698, M. Lystrup, H. A. MacEwen, and G. G. Fazio Eds., Proceedings of SPIE, 2018.

[13] S. Martin, M. Rud, D. Mawet, J. Nissen, S. Shaklan, and L. Marchen, "HabEx Space Telescope Exoplanet Instruments," in *Space Telescopes and Instrumentation 2018: Optical, Infrared, and Millimeter Wave*, vol. 10698, M. Lystrup, H. A. MacEwen, and G. G. Fazio Eds., Proceedings of SPIE, 2018.

[14] S. Martin, M. Rud, P. Scowen, D. Stern, and J. Nissen, "HabEx Space Telescope Optical System Overview: General Astrophysics Instruments," in *Space Telescopes and Instrumentation 2018: Optical, Infrared, and Millimeter Wave*, vol. 10698, M. Lystrup, H. A. MacEwen, and G. G. Fazio Eds., Proceedings of SPIE, 2018.

[15] A. J. E. Riggs, G. Ruane, K. Fogarty, L. Pueyo, and K. Balasubramanian, "Numerically Optimized Coronagraph Designs for the Habitable Exoplanet Imaging Mission (HabEx) Concept," in *Conference on Space Telescopes and Instrumentation - Optical, Infrared, and Millimeter Wave*, Austin, TX, Jun 10-15 2018, vol. 10698, BELLINGHAM: Spie-Int Soc Optical Engineering, in Proceedings of SPIE, 2018, doi: 10.1117/12.2313843. [Online]. Available: <Go to ISI>://WOS:000450864600025

[16] J. Wang, D. Mawet, R. Y. Hu, G. Ruane, J. R. Delorme, and N. Klimovich, "Baseline requirements for detecting biosignatures with the HabEx and LUVOIR mission concepts," *Journal of Astronomical Telescopes Instruments and Systems,* vol. 4, no. 3, Jul 2018, Art no. 035001, doi: 10.1117/1.jatis.4.3.035001.

[17] I. J. E. Jordan *et al.*, "Enhancing NGST Science: UMBRAS," in *Next Generation Space Telescope Science and Technology*, January 01, 2000, vol. 207, p. 468. [Online]. Available: https://ui.adsabs.harvard.edu/abs/2000ASPC..207..468J

[18] C. J. Copi and G. D. Starkman, "The Big Occulting Steerable Satellite (BOSS)," *The Astrophysical Journal,* vol. 532, pp. 581-592, March 01, 2000.

[19] W. Cash, "Detection of Earth-like planets around nearby stars using a petal-shaped occulter," *Nature,* vol. 442, pp. 51-53, July 01, 2006.

[20] W. Cash, "Analytic Modeling of Starshades," *The Astrophysical Journal,* vol. 738, September 01, 2011.

[21] N. J. Kasdin *et al.*, "Occulter design for THEIA," in *Techniques and Instrumentation for Detection of Exoplanets IV*, August 01, 2009, vol. 7440. [Online]. Available: https://ui.adsabs.harvard.edu/abs/2009SPIE.7440E..05K

[22] C. A. Crow *et al.*, "Views from EPOXI: Colors in Our Solar System as an Analog for Extrasolar Planets," *The Astrophysical Journal,* vol. 729, March 01, 2011.

[23] J. H. Madden and L. Kaltenegger, "A Catalog of Spectra, Albedos, and Colors of Solar System Bodies for Exoplanet Comparison," *Astrobiology,* vol. 18, pp. 1559-1573, December 01, 2018.

[24] C. M. Guimond and N. B. Cowan, "The Direct Imaging Search for Earth 2.0: Quantifying Biases and Planetary False Positives," *Astronomical Journal,* vol. 155, no. 6, Jun 2018, Art no. 230, doi: 10.3847/1538-3881/aabb02.

[25] C. M. Guimond and N. B. Cowan, "Three Direct Imaging Epochs Could Constrain the Orbit of Earth 2.0 inside the Habitable Zone," *The Astronomical Journal,* vol. 157, May 01, 2019.

[26] G. L. Villanueva, M. D. Smith, S. Protopapa, S. Faggi, and A. M. Mandell, "Planetary Spectrum Generator: An accurate online radiative transfer suite for atmospheres, comets, small bodies and exoplanets," *Journal of Quantitative Spectroscopy and Radiative Transfer,* vol. 217, pp. 86-104, September 01, 2018.

[27] A. Jones, S. Noll, W. Kausch, C. Szyszka, and S. Kimeswenger, "An advanced scattered moonlight model for Cerro Paranal," *Astronomy and Astrophysics,* vol. 560, December 01, 2013.

[28] S. Noll *et al.*, "An atmospheric radiation model for Cerro Paranal I. The optical spectral range," *Astronomy & Astrophysics,* vol. 543, Jul 2012, Art no. A92, doi: 10.1051/0004-6361/201219040.

[29] W. H. J. Childs, "Equivalent widths in the A and B bands of oxygen," *Astrophysical Journal,* vol. 77, no. 3, pp. 212-220, Apr 1933, doi: 10.1086/143459.

[30] C. Stark, "Optimal Architectures and Survey Designs for Maximizing the Yields of Direct-Imaging Exoplanet Missions.," ed. Astro2020 Decadal Survey White Paper: National Academy of Sciences, 2019.

[31] R. J. Vanderbei, E. Cady, and N. J. Kasdin, "Optimal Occulter Design for Finding Extrasolar Planets," *The Astrophysical Journal,* vol. 665, pp. 794-798, August 01, 2007.

[32] J.-L. Beuzit *et al.*, "SPHERE: the exoplanet imager for the Very Large Telescope," *arXiv e-prints,*

[33] H. M. Schmid *et al.*, "SPHERE/ZIMPOL high resolution polarimetric imager," (in English), *Astronomy & Astrophysics,* Article vol. 619, p. 37, Nov 2018, Art no. A9, doi: 10.1051/0004-6361/201833620.

[34] L. M. Close *et al.*, "Status of MagAO and review of astronomical science with visible light adaptive optics," in *Conference on Adaptive Optics Systems VI*, Austin, TX, Jun 10-15 2018, vol. 10703, in Proceedings of SPIE, 2018, doi: 10.1117/12.2313107. [Online]. Available: <Go to ISI>://WOS:000452819300018

[35] J. Males *et al.*, "MagAO-X: project status and first laboratory results," (in English), *Adaptive Optics Systems Vi,* Proceedings Paper vol. 10703, 2018, Art no. UNSP 1070309, doi: 10.1117/12.2312992.

[36] O. Guyon, "Extreme Adaptive Optics," *Annual Review of Astronomy and Astrophysics,* vol. 56, no. 1, pp. 315-355, 2018, doi: 10.1146/annurev-astro-081817-052000.

[37] W. A. Marlow *et al.*, "Laser-Guide-Star Satellite for Ground-Based Adaptive Optics Imaging of Geosynchronous Satellites," *Journal of Spacecraft and Rockets,* vol. 54, pp. 621-639, May 01, 2017 2017.